BASIC RESEARCH www.jasn.org

Endothelin-1 Inhibits the Epithelial Na^+ Channel through βPix/14-3-3/Nedd4-2

Tengis S. Pavlov,* Ahmed Chahdi,† Daria V. Ilatovskaya,*‡ Vladislav Levchenko,* Alain Vandewalle,§ Oleh Pochynyuk,‖ Andrey Sorokin,†¶ and Alexander Staruschenko*¶

Departments of *Physiology and †Medicine, and ¶Kidney Disease Center, Medical College of Wisconsin, Milwaukee, Wisconsin; ‡Institute of Cytology, Russian Academy of Sciences, St. Petersburg, Russian Federation; §Institut National de la Santé et de la Recherche Médicale Unit 773, Centre de Recherche Biomédicale Bichat-Beaujon, Université Paris 7-Denis Diderot, Paris, France; and ‖Department of Physiology, University of Texas Health Science Center at San Antonio, San Antonio, Texas

ABSTRACT

Epithelial Na^+ channels (ENaCs) mediate sodium reabsorption in the cortical collecting duct (CCD), but the regulatory pathways that modulate the activity of these channels are incompletely understood. Here, we observed that endothelin-1 (ET-1) attenuates ENaC activity acutely by reducing the channel's open probability and chronically by decreasing the number of channels in the plasma membrane. To investigate whether β_1Pix, a signaling protein activated by ET-1, mediates ENaC activity, we reconstituted ENaC in CHO cells with or without coexpressed β_1Pix and found that β_1Pix negatively regulates ENaC. Knockdown of βPix in native principal cells abolished the ET-1-induced decrease in ENaC channel number. Furthermore, we found that βPix does not decrease ENaC activity through its guanine nucleotide exchange factor (GEF) activity for Rac1 and Cdc42. Instead, coexpression of β_1Pix mutant constructs revealed that β_1Pix affects ENaC activity through binding 14-3-3 proteins. Coimmunoprecipitation experiments supported a physical interaction between β_1Pix and 14-3-3β in cultured principal cells. Coexpression of 14-3-3β increased ENaC activity in CHO cells, but concomitant expression of β_1Pix attenuated this increase. Recruitment of 14-3-3β by β_1Pix impaired the interaction of 14-3-3β with the ubiquitin ligase Nedd4-2, thereby promoting ubiquitination and degradation of ENaC. Taken together, these results suggest that the inhibitory effects of chronic ET-1 on ENaC result from βPix interacting with the 14-3-3/Nedd4-2 pathway.

J Am Soc Nephrol 21: 833–843, 2010. doi: 10.1681/ASN.2009080885

Maintenance of water-electrolyte balance by the kidneys is an important mechanism of body fluid volume and BP regulation. The long-term control of BP involves Na^+ homeostasis through the precise regulation of the epithelial Na^+ channel (ENaC) in the aldosterone-sensitive distal nephron. Abnormalities in ENaC function have been linked to disorders of: total body Na^+ homeostasis, blood volume, BP, and lung fluid balance.[1,2] For example, a partial loss-of-function mutation of ENaC produces pseudohypoaldosteronism type 1,[3,4] characterized by salt wasting. In contrast, a gain-of-function mutation leads to Liddle syndrome.[5–7]

Endothelin-1 (ET-1) is a powerful vasoactive peptide[8] that controls cell proliferation and gene expression and may also be an important negative regulator of sodium and water reabsorption.[9–11]

Received August 31, 2009. Accepted January 22, 2010.

Published online ahead of print. Publication date available at www.jasn.org.

Correspondence: Dr. Alexander Staruschenko, Department of Physiology, Medical College of Wisconsin, 8701 Watertown Plank Road, Milwaukee, WI 53226. Phone: 414-955-8475; Fax: 414-955-6546; E-mail: Staruschenko@mcw.edu; or Dr. Andrey Sorokin, Department of Medicine/Nephrology, Medical College of Wisconsin, 8701 Watertown Plank Road, Milwaukee, WI 53226. Phone: 414-456-4438; Fax: 414-456-6312; E-mail: Sorokin@mcw.edu

ET-1 targets cells through ET_A and ET_B receptors. Collecting duct (CD)-specific knockout of ET-1 causes hypertension. CD-specific knockout of the ET_A receptor does not alter BP, whereas CD-specific knockout of the ET_B receptor increases BP to a lesser extent than CD ET-1 knockout.[12–14] Combined knockout of CD ET_A and ET_B receptors causes hypertension and sodium retention.[15] ET_B-knockout rats develop hypertension on a high-salt diet. Normal BP in these salt-sensitive, hypertensive rats is restored after amiloride treatment.[16] Moreover, electrophysiological study showed that picomolar concentrations of ET-1 attenuate ENaC open probability via ET_B receptors in an amphibian distal nephron cell line.[17] Similar results were demonstrated in mammalian fibroblast cells by stably expressing genes for the three ENaC subunits. The inhibitory effect of ET-1 on ENaC could be completely blocked when cells were pretreated with the selective Src family kinase inhibitor, PP2. Further studies revealed that basal Src family kinase activity strongly regulates ENaC inhibition.[18] Bugaj *et al.* [19] recently demonstrated in native rat cortical collecting duct (CCD) principal cells that ET-1 dynamically decreases ENaC open probability via ET_B receptors and that subsequent intracellular pathways involved Src tyrosine kinase activity and MAPK1/2 signaling. Furthermore, it was recently shown that aldosterone modulates steroid receptor binding to the ET-1 gene.[20]

Our previous studies showed that several small G proteins, including K-Ras, RhoA, and Rab11a, alter ENaC activity.[21–26] The activity of small G proteins is modulated by guanine nucleotide exchange factors (GEFs). p21-activated kinase (Pak)-interacting exchange factor β (βPix) is a member of the DBL (diffuse B cell lymphoma) family of Rho-GEFs for Rac1 and Cdc42. We have shown previously that ET-1 induces β_1Pix translocation to focal adhesions through a PKA-dependent pathway[27] and that β_1Pix plays a crucial role in the regulation of Cdc42 activation by ET-1.[28] Moreover, we have reported up-regulation of βPix expression by ET-1 in primary human mesangial cells and identified a number of signaling molecules that form a multiunit signaling complex with βPix.[29] Consequently, βPix plays an important role in ET-1 signal transduction and possesses both GEF and scaffolding activity.

Using tagged 14-3-3 proteins, Jin *et al.*[30] showed for the first time that βPix can bind 14-3-3 proteins. Later, Angrand and colleagues [31] used tandem affinity purification and liquid chromatography-mass spectrometry methods to confirm 14-3-3 binding with βPix. We have recently provided a mechanistic insight into the role of 14-3-3β in modulating β_1Pix activity and identified 14-3-3β-binding sites on β_1Pix.[32] 14-3-3 proteins are essential components of ENaC regulation. These proteins associate with SGK1-phosphorylated Nedd4-2 to maintain its phosphorylated/inactive state and thereby obstruct its physical association with ENaC.[33–37]

In the present study we report that ET-1 significantly decreases ENaC activity in three different cell types, including freshly isolated rat CCD. Furthermore, we demonstrate here that βPix is highly expressed in various cell lines, localized in CCD, and decreases ENaC activity when coexpressed in Chinese hamster ovary (CHO) cells. This effect did not occur through β_1Pix GEF activity and was mediated by binding with 14-3-3 proteins. βPix silencing demonstrated that βPix is not involved in the acute effect of ET-1 on channel open probability but instead mediates chronic decrease of number of active channels. These results reveal a new signaling pathway that brings together several proteins known to play a central role in the regulation of ENaC. Furthermore, these findings identify novel pathway for GEF βPix action in which scaffolding activity, but not GEF activity, controls negative regulation of signaling independent of small G protein activation. Thus, our data suggest the existence of signaling pathway initiated by ET-1 and resulting in down-regulation of ENaC activity by βPix which acts via 14-3-3/Nedd4-2 complex.

RESULTS

ET-1 Decreases ENaC Activity in a Biphasic Pattern: An Acute and a Chronic Phase

In the present study we tested the effect of ET-1 on ENaC activity in three different cell types. First, we isolated CDs, split them open, and formed cell-attached seals on the apical membrane of principal cells to directly monitor changes in ENaC activity in real time. The representative current recording in Figure 1A documents the time course of inhibiting ENaC activity in freshly isolated rat CCDs. A continuous trace before and after addition of 20 nM of ET-1 is shown at the top. Segments before and after ET-1 are shown below at expanded time scales. The effect of ET-1 was partially reversible, with channel activity quickly recovering upon washout of ET-1 (Figure 1A). Similarly, ET-1 (100 nM) rapidly decreased ENaC activity in cell-attached experiments on mouse cortical CD principal ($mpkCCD_{c14}$) cells and CHO cells transiently transfected with all three ENaC subunits and ET_BR (Figure 1, B and C). As summarized in Figure 1D, ET-1 acutely decreased ENaC open probability (P_o) in all three studied cell systems.

After 24-hour treatment of $mpkCCD_{c14}$ cells with 100 nM ET-1, we also observed decrease in ENaC activity (Figure 2). However, underlying mechanisms of acute and chronic effects of ET-1 treatment are remarkably different. Acute effect was mediated by decreases in channel P_o, whereas long-term effect was mediated by decrease in the number of channels. When $mpkCCD_{c14}$ cells were pretreated with ET-1 for 24 hours, P_o did not significantly change (0.60 ± 0.10 and 0.48 ± 0.10 before and after treatment, respectively). In contrast, chronic treatment with ET-1 (24 hours) resulted in significant decrease of number of observed channels (N) (from 2.57 ± 0.48 to 1.38 ± 0.26). These results demonstrate that ET-1 regulates ENaC in two phases: an acute phase mediated by decreasing P_o and a chronic phase resulting in a decrease of the number of channels in the plasma membrane.

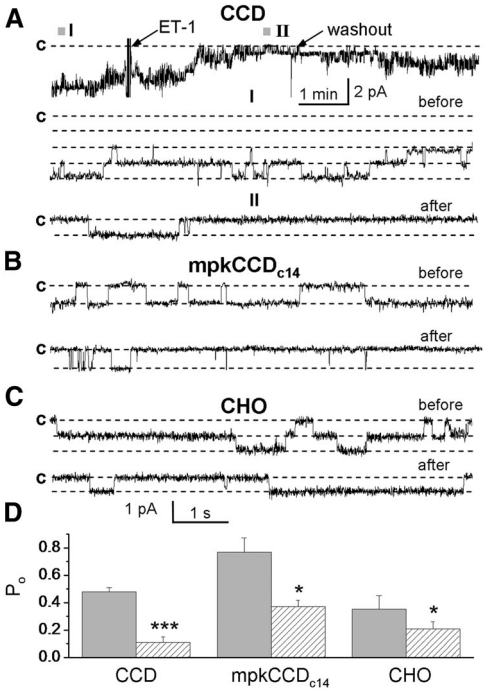

Figure 1. ET-1 acutely decreases ENaC activity. (A) Continuous current trace from a representative cell-attached patch that contained at least four ENaCs and was made on the apical membrane of principal cells in isolated split-open rat CD before and after treatment with ET-1 (20 nM). Areas before (I) and after (II) treatment are shown below with an expanded time scale. This patch was held at a −60 mV test potential during the course of the experiment. c denotes closed current level. Dashed lines denote closed and open current levels. (B and C) Current traces from representative cell-attached patches that contained ENaCs and were made on the apical membrane of mpkCCD$_{c14}$ cells (B) or from CHO cells overexpressed with all three ENaC subunits (C) before and after treatment with ET-1 (100 nM). Patches were held at test potentials of −60 mV during the course of these experiments. (D) Summary graphs of P_o in cell-attached patches from freshly isolated CCD, mpkCCD$_{c14}$, or transiently transfected CHO cells before (light gray bars) and after (patterned bars) ET-1. Data are mean ± SEM. Asterisks indicate *versus* before application of ET-1.

βPix Expression and Localization

We have previously shown that exposure to ET-1 stimulation induced βPix expression and activation of βPix's mediated signaling cascades.[27,29] Thus, we were interested in testing the hypothesis that βPix is involved in ET-1-mediated decrease in ENaC activity. Immunohistochemistry analysis was performed in Sprague-Dawley rat kidneys to identify a distribution of βPix protein. Figure 3A demonstrates a representative immunohistochemistry staining for βPix at 20× (upper panels) and 40× (lower panels) magnifications. Negative controls (left) (stained without primary and secondary antibodies) are also shown. Additional negative control (staining with secondary antibodies in the absence of primary antibodies) also did not show any staining (data not shown).

Western blot analysis identified expression of endogenous βPix in various cell lines. The data presented in Figure 3B show expression of βPix in human mesangial and renal carcinoma 786-O cells, CHO cells, differentiated mouse cortical CD principal cells (mpkCCD$_{c14}$ and M-1), Madin-Darby canine kidney cells, and renal proximal tubule epithelial cells. These results demonstrate that βPix is expressed in various cultured cell lines, including principal cells, *in vitro* and is detected in CCD *in vivo*.

β_1Pix Decreases ENaC Activity

To investigate the actions of β_1Pix on ENaC we reconstituted the channel in CHO cells in the absence and presence of coexpressed β_1Pix. Figure 4A shows ENaC currents before (arrows) and after treatment with amiloride (10 μM), which is a well-known inhibitor of channels in the ENaC/DEG family in a cell expressing the channel alone (up) and in a cell expressing both the channel and wild-type β_1Pix. Currents were elicited by voltage ramping from 60 mV down to −100 mV (holding potential at 40 mV). As summarized in Figure 4B, coexpression of β_1Pix markedly decreased ENaC current density from 374 ± 29 to 149 ± 20 pA/pF. CHO cells, transfected with vector encoding wild-type β_1Pix, demonstrated a level of β_1Pix expression much higher than the endogenous βPix level (Figure 4C). Expression levels of myc-ENaC in CHO cells transfected with either control vector or vector encoding β_1Pix were similar (data not shown). Thus, our data are the first demonstration of negative regulation of ENaC by β_1Pix.

βPix Is Involved in Long-Term Inhibition of ENaC by ET-1

Because both ET-1 and βPix decrease ENaC activity and previous published results support coupling between ET-1 signaling and βPix, we were interested in testing whether βPix is involved in ET-1 effects on ENaC. To establish a role of βPix in

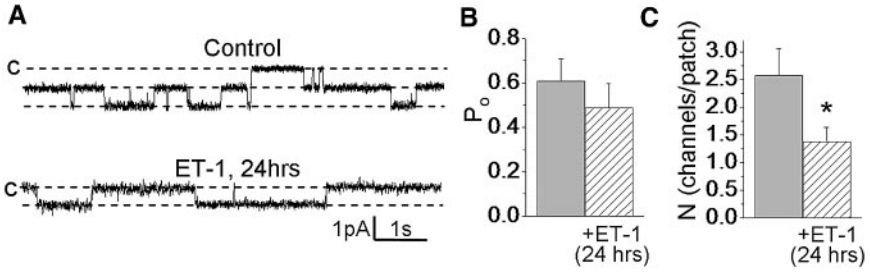

Figure 2. ET-1 chronically decreases ENaC activity. (A) Representative current traces from cell-attached patches that contained ENaCs and were made on the apical membrane of mpkCCD$_{c14}$ cells not treated (control) and treated with ET-1 (100 nM; 24 h). (B and C) Summary graphs showing the chronic effects of ET-1 on ENaC P_o (B) and the mean number of ENaCs within patches (C) under each condition. Asterisks indicate *versus* without treatment.

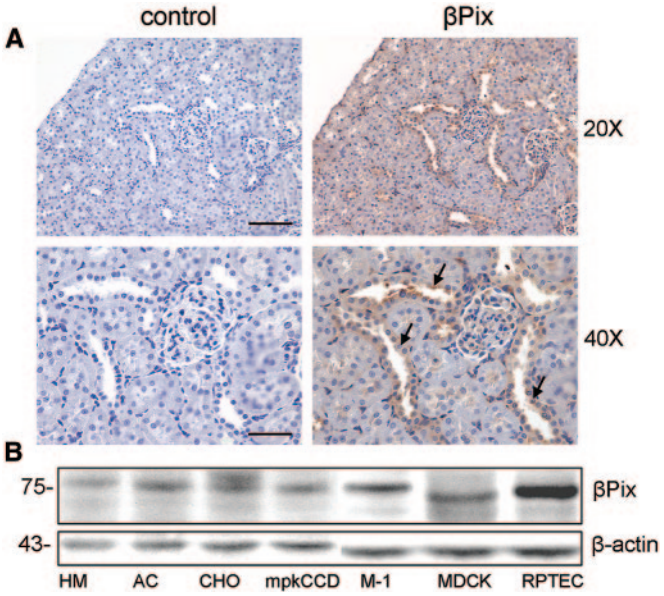

Figure 3. βPix is expressed in rat kidney tissue and in a variety of cell lines. (A) Representative immunohistochemical staining for βPix detection (right) in kidney cortical sections of Sprague-Dawley rat. Original magnifications, ×20 (upper; scale bar: 100 μm) and ×40 (lower; scale bar: 50 μm). Negative controls (left) (stained without primary and secondary antibodies) are also shown. (B) Western blot analysis of cultured mammalian cells reveals the ubiquitous expression of βPix. The data presented for proteins extracted from immortalized human mesangial cells (HM), human renal carcinoma 786-O cells (AC), CHO cells, immortalized mouse cortical collecting duct principal cells (mpkCCD$_{c14}$ and M-1), Madin-Darby canine kidney cells, and renal proximal tubule epithelial cells (RTEC). Equal amount of protein loaded in each lane was verified by Western blotting with anti-actin antibodies. Western blot analysis was repeated twice with similar results.

ET-1-mediated down-regulation of ENaC activity, we used shRNA against βPix. Mouse βPix shRNA lentiviral particles were used to down-regulate mRNA levels of βPix in mpkCCD$_{c14}$ cells. Efficient down-regulation of βPix expression in mpkCCD$_{c14}$ cells treated with βPix shRNA lentivirus (but not with control lentivirus) was verified by Western blot analysis (Figure 5A). Next, we examined functional consequences of βPix silencing using cell-attached seals on the apical membrane of mpkCCD$_{c14}$ principal cells with βPix-introduced shRNA, to directly monitor acute changes in ENaC activity in response to ET-1 in real time. As summarized in Figure 5B, ENaC activity was significantly decreased in response to acute application of ET-1, similar to wild-type mpkCCD$_{c14}$ cells (Figure 1, B and D). The mean number of active channels within patches was unchanged. These results demonstrate that βPix is not involved in acute decrease of ENaC activity in mpkCCD$_{c14}$ cells. Next, we tested the chronic effect of ET-1 on ENaC activity in βPix-depleted mpkCCD$_{c14}$ cells. For these experiments, cells were treated for 24 hours with 100 nM ET-1. As shown in Figure 5C, in the absence of βPix, chronic treatment with ET-1 did not decrease ENaC activity. On the contrary, ET-1 significantly decreased ENaC activity in mpkCCD$_{c14}$ cells infected with lentivirus encoding scrambled shRNA, the same way long-term ET-1 treatment did in wild-type mpkCCD$_{c14}$ cells (Figure 2). Thus, βPix is involved in chronic decrease of the number of active channels in response to ET-1 treatment.

Rac1 and Cdc42 Are Not Involved in β_1Pix-Dependent Decrease in ENaC Activity

β_1Pix was shown to be a GEF for Rac1 and Cdc42.[38,39] Moreover, we and others have shown previously that several small G proteins regulate ENaC activity through different mechanisms. Thus, we tested the effect of Rac1 and Cdc42 on ENaC activity in CHO cells. Rac1 markedly enhanced ENaC activity. Coexpression of ENaC subunits with wild-type or constitutively active (QL) Rac1 significantly increased ENaC activity from 215 ± 17 to 530 ± 86 and 657 ± 96 pA/pF, respectively. Surprisingly, coexpression of neither wild-type nor constitutively active (G12V) mutant Cdc42 had an effect on ENaC activity (Figure 6). These results suggest that β_1Pix decreases ENaC activity through a mechanism not involving GEF activity for Rac1 and Cdc42.

14-3-3β and Nedd4-2 Involvement in β_1Pix Regulation of ENaC Activity

We have previously described two mutants of β_1Pix: β_1Pix Δ602 to 611 and L238R, L239R, which affect β_1Pix scaffolding and GEF activity, respectively. β_1Pix (Δ602 to 611) has amino acid residues 602 to 611, located within the leucine zipper do-

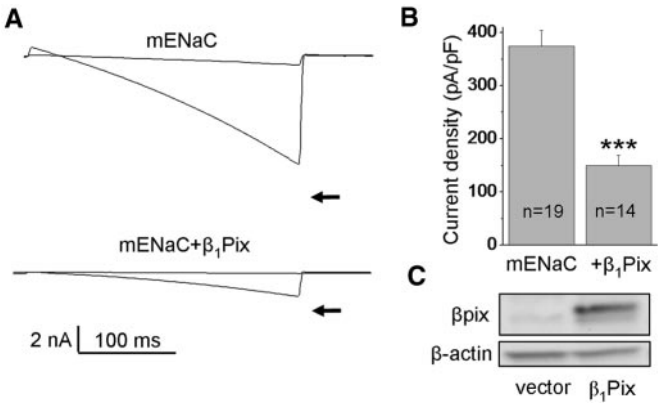

Figure 4. β_1Pix decreases ENaC activity. (A) Overlays of typical macroscopic current traces before (arrow) and after 10 μM amiloride from voltage-clamped CHO cells transfected with mENaC alone (top) and with β_1Pix (bottom). Currents evoked with a voltage ramp (60 to −100 mV from a holding potential of 40 mV). (B) Summary graph of the mean ± SEM amiloride-sensitive current density at −80 mV for voltage-clamped CHO cells expressing mENaC in the absence and presence of β_1Pix. The numbers of observations for each group are shown. Asterisks indicate *versus* ENaC alone. (C) Expression levels of βPix in CHO cells transfected with either control vector (vector) or vector encoding β_1Pix (β_1Pix). Cell lysates were analyzed using anti-βPix antibodies (upper). Equal loading was verified by anti-actin antibodies (lower). Data shown are representative of three experiments.

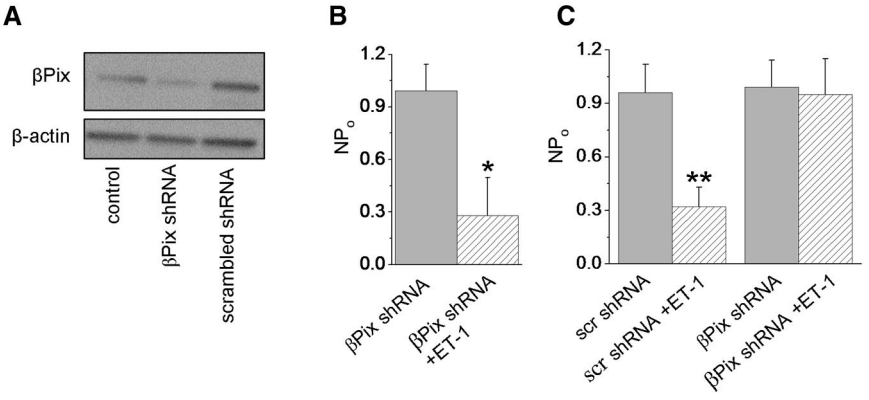

Figure 5. βPix is involved in the long-term effect of ET-1 on ENaC activity. (A) Western blot from wild-type (control) mpkCCD$_{c14}$ cells or cells expressing either shRNAs *versus* βPix or scrambled shRNA. Cell lysates were analyzed using anti-βPix antibodies (upper). Equal loading was verified by anti-actin antibodies (lower). Shown are representative data from three experiments. (B and C) Summary graphs showing acute (B) and long-term (C) effects of ET-1 (100 nM) on ENaC activity (NP$_o$). The number of patches assessed for each group is shown. Data are mean ± SEM. Asterisks indicate *versus* before ET-1.

main, deleted, and their deletion interferes with β_1Pix homodimerization. 14-3-3 binding requires β_1Pix homodimerization, and deletion of amino acids 602 to 611 completely inhibited the interaction between 14-3-3β and β_1Pix.[32] β_1Pix (L238R, L239R) mutant contains an inactive DH domain and lacks GEF activity.[27,38] As summarized in Figure 7A, coexpression of wild-type β_1Pix and β_1Pix (L238R, L239R) DH mutant but not β_1Pix (Δ602 to 611) mutant in CHO cells significantly decreased ENaC activity. Furthermore, we tested whether the lower current magnitude was due to different expression of β_1Pix constructs. To that end, we performed Western blot analysis of β_1Pix proteins from CHO cells transfected with empty vector, myc-tagged wild-type, β_1Pix (L238R, L239R) or β_1Pix (Δ602 to 611) mutants. The protein products were detected at comparable levels in all three groups (Figure 7B). We interpret these results as an evidence that β_1Pix affected ENaC activity via 14-3-3 binding but not GEF activity.

To further understand how β_1Pix regulates ENaC activity, we tested whether β_1Pix interacts with 14-3-3β in mpkCCD$_{c14}$ principal cells. As shown in Figure 8A, endogenous 14-3-3β is coimmunoprecipitated with βPix in mpkCCD$_{c14}$ cells. Cell lysates were subjected to immunoprecipitation using anti-14-3-3β antibodies. Immunoprecipitated 14-3-3β and coprecipitated βPix were detected using anti-14-3-3β and anti-βPix antibodies, respectively. Results shown in Figure 8B are also consistent with β_1Pix and 14-3-3β being parts of the same signaling cascade with respect to ENaC. In these experiments we coexpressed mENaC in CHO cells either alone or in combination with 14-3-3β and β_1Pix separately or together. Coexpression of 14-3-3β significantly increased ENaC activity. However, ENaC activity was significantly decreased when β_1Pix was coexpressed with 14-3-3β. These results clearly show that β_1Pix is involved in 14-3-3β-mediated regulation of ENaC activity.

To determine the physiologic significance of 14-3-3β binding to β_1Pix and its role in Nedd4-2 regulation, we sought to investigate the effect of β_1Pix overexpression upon ability of 14-3-3 to interact with Nedd4-2. To this end, cells were transfected with plasmid encoding FLAG-tagged Nedd4-2, and coimmunoprecipitation of 14-3-3β with Nedd4-2 was evaluated in the presence and absence of overexpressed β_1Pix (Figure 9). In the absence of overexpressed β_1Pix, coimmunoprecipitation of 14-3-3 with anti-FLAG antibodies was detected, as expected. Coprecipitation of 14-3-3 with Nedd4-2 was not observed when β_1Pix was coexpressed (Figure 9C). These data suggest that β_1Pix recruitment of 14-3-3β decreases interaction of 14-3-3β with Nedd4-2. Moreover, βPix has no effect on ENaC activity when coexpressed with dominant negative Nedd4-2 as assessed by electrophysiology (Figure 10A). Furthermore, βPix's effect is abolished by overexpression of Liddle syndrome mutants of ENaC (Figure 10B). In these experiments we coexpressed ENaC subunits with three prolines (3P) mutated to Ala in the PY motif in the absence and presence of β_1Pix. Furthermore, we and others have shown previously that the conserved Thr628 preceding the PY motif in γ-ENaC, similar to the PY motif in this subunit, has an effect on interactions with Nedd4-2.[40,41] Phosphorylation of this site has previously been reported to enhance the interaction of ENaC and Nedd4.[42] As apparent in Figure 10, B and C, overexpression of β_1Pix with ENaC mutants required for the Nedd4-2 regulation had no effect on

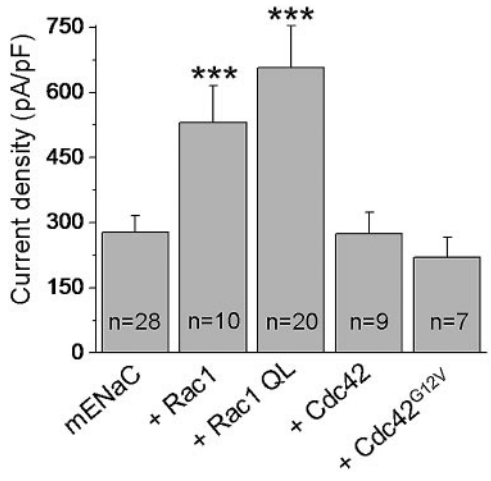

Figure 6. Regulation of ENaC activity by small G proteins Rac1 and Cdc42. Summary graph of ENaC activity measured in whole-cell voltage-clamp experiments from CHO cells expressing ENaC alone and the channel plus wild-type and constitutively active Rac1 (QL) or Cdc42 (G12V). The numbers of observations for each group are shown. Asterisks indicate *versus* mENaC alone.

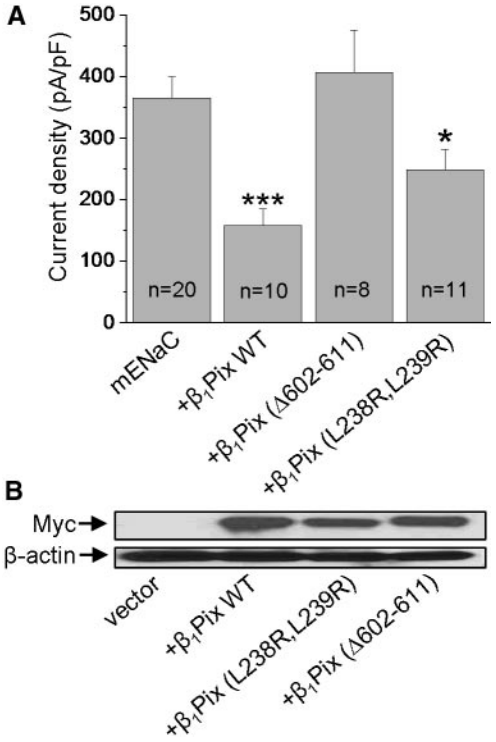

Figure 7. β_1Pix mediates ENaC activity through a mechanism that does not involve GEF activity for Rac1 and Cdc42. (A) Summary graph of ENaC activity measured in whole-cell voltage-clamp experiments from CHO cells expressing channel alone and channel plus wild-type and mutant (Δ602 to 611 or L238R, L239R) β_1Pix. Asterisk indicates *versus* mENaC alone. (B) Western blot analysis of βPix expression in CHO cells transfected with either empty vector or Myc-tagged wild-type and mutant β_1Pix. Cell lysates were analyzed using anti-Myc antibodies (upper). Equal loading was verified by anti-actin antibodies (lower). Shown is the representative of three experiments.

channel activity. This finding adds additional support to our hypothesis that β_1Pix decreases ENaC activity by involving the 14-3-3/Nedd4-2 signaling pathway.

DISCUSSION

The activity of ENaC is under the control of a number of regulatory mechanisms and signaling molecules. ET-1, 14-3-3, and Nedd4-2 are known to play a central role in the regulation of ENaC. Our data identify a new signaling pathway that brings together all cited above signaling proteins. Shown in Figure 11 is a possible model for regulation of ENaC by ET-1 via a βPix/14-3-3/Nedd4-2 complex. We propose that an ET-1-mediated complex between βPix and 14-3-3 facilitates Nedd4-2 binding to ENaC, thereby decreasing ENaC activity via affecting the number of active channels.

Some data support a role for ET-1 regulation of ENaC, most likely via ET_B receptors.[17–19] Renal tubular cells may secrete ET-1 themselves, which could regulate sodium transport in the kidney under physiologic and pathologic conditions. Our observations that ET-1 decreases ENaC activity in freshly isolated principal cells of the rat CD, polarized mouse $mpkCCD_{c14}$ cells, and CHO cells transiently expressed with ENaC subunits, are consistent with those data. Furthermore, we have shown that ET-1 regulates ENaC in a biphasic pattern, and that long-term effect is mediated by decreasing in the number of channels.

β_1Pix is a GEF for Rac1 and Cdc42.[38] Coexpression of β_1Pix with ENaC decreased amiloride-sensitive current in CHO cells. We expected that β_1Pix modulates ENaC activity via activation of Rac1 and Cdc42 small G proteins. However, the effect of β_1Pix is unlikely to occur through GEF activity of β_1Pix, because dimerization-deficient β_1Pix mutant failed to decrease ENaC activity while retaining GEF activity toward Cdc42. Although dimerization-deficient β_1Pix mutant has diminished GEF activity toward Rac1, involvement of this small GTPase in regulation of ENaC in our experimental system could be ruled out on the basis of our experiments with constitutively active mutant of Rac1. Furthermore, a β_1Pix mutant that has no GEF activity decreased current density to a similar extent as wild-type β_1Pix. Several lines of evidence suggest that β_1Pix acts not only as GEF for Rac1 and Cdc42, but also as a scaffolding protein. For example, we have recently demonstrated that ET-1 stimulation of primary human mesangial cells induces βPix and p66Shc up-regulation, resulting in the formation of the βPix/p66Shc complex.[29] In our current and previous studies,[32] we have further explored the interaction between 14-3-3β and β_1Pix using coimmunoprecipitation studies. Moreover, we have shown that there is less interaction of 14-3-3 with Nedd4-2 when coexpressed with βPix. 14-3-3 proteins modulate the expression of ENaC by phosphorylation-dependent interaction with Nedd4-2.[33,34] Aldosterone selectively increased 14-3-3 protein isoform expression, and as-

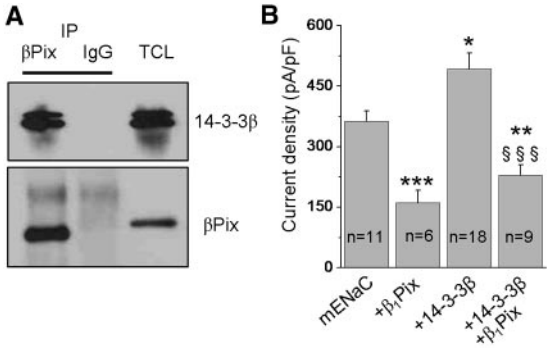

Figure 8. 14-3-3β binds to β_1Pix and is involved in the effect of β_1Pix on ENaC activity. (A) Lysates from $mpkCCD_{c14}$ principal cells were immunoprecipitated (IP) with anti-βPix or IgG control followed by immunoblotting with anti-βPix or anti-14-3-3β antibodies. Also shown are expression levels of 14-3-3β and βPix in total cell lysates (TCL). (B) Summary graph of ENaC activity measured in whole-cell voltage-clamp experiments from CHO cells expressing channel alone, channel plus 14-3-3β, and β_1Pix separately and together. Data are mean ± SEM. Asterisk indicates *versus* ENaC alone. §, *versus* ENaC plus 14-3-3.

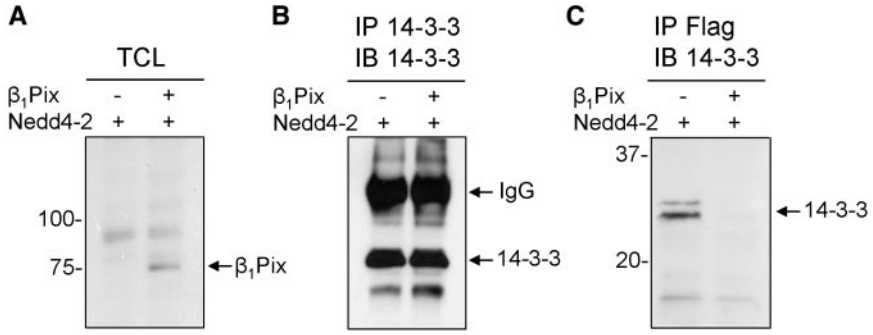

Figure 9. β_1Pix recruitment of 14-3-3β decreases interaction of 14-3-3β with Nedd4-2. CHO cells were transfected with plasmid encoding FLAG-tagged Nedd4-2 and cotransfected with either control plasmid (−) or plasmid encoding Myc-tagged β_1Pix (+). (A) Lysates from CHO cells were analyzed by Western blotting using anti-Myc antibodies to verify β_1Pix expression. (B) Equal expression of 14-3-3β was verified using immunoprecipitation (IP) with anti-14-3-3β antibodies followed by Western blotting with anti-14-3-3β antibodies. (C) Lysates from CHO cells were immunoprecipitated with anti-FLAG antibodies followed by Western blotting with anti-14-3-3β antibodies. The band recognized by 14-3-3β antibodies corresponds to 14-3-3β coprecipitated with Nedd4-2. Overexpression of β_1Pix efficiently prevents coprecipitation of 14-3-3β with Nedd4-2. TCL, total cell lysate; IB, immunoblot.

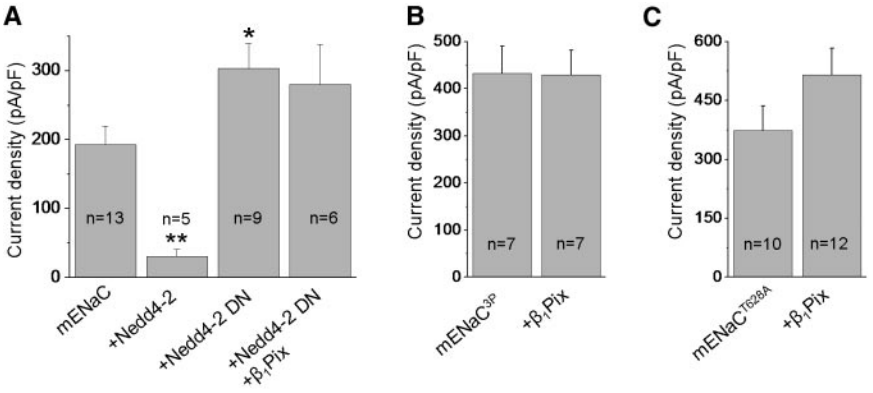

Figure 10. β_1Pix down-regulates ENaC activity via Nedd4-2. (A) Summary graph of ENaC activity measured in whole-cell voltage-clamp experiments from CHO cells expressing ENaC alone and the channel plus wild-type and dominant-negative Nedd4-2 alone or coexpressed with β_1Pix. The numbers of observations for each group are shown. Asterisk indicates *versus* mENaC alone. (B and C) Summary graph of the effect of β_1Pix on activity of ENaC having Liddle syndrome mutants (mutation of the three prolines in the PY motif; 3P) in all three ENaC subunits (B) and the T628A mutation in γ-subunit (C). The number of patches assessed for each group is shown.

sociation of 14-3-3 with phospho-Nedd4-2 is required for sodium transport stimulation.[35,36]

A mechanism by which Sgk affects ENaC activity by disrupting Nedd4-2 binding to the channel is well documented. Sgk1 and Nedd4-2 converge into a common cell signaling pathway and regulate the cell surface density of ENaC, where Sgk1 phosphorylates Nedd4-2, thereby reducing both its binding affinity to ENaC and the rate of ENaC degradation.[43–46] It is unclear at this time whether Nedd4-2, SGK, 14-3-3, and β_1Pix have roles at different sites along a common trafficking pathway or are components of distinct trafficking pathways with respect to ENaC. Regardless of whether these trafficking proteins are involved in one or more pathways of ENaC regulation, we can state that β_1Pix forms a complex with 14-3-3 and negatively regulates ENaC activity. Most likely, ET-1 through basolateral ET_BR rapidly decreases ENaC open probability through a signaling cascade involving activation of src family tyrosine kinases and stimulation of its downstream MAPK1/2 effector cascade. Later, ET-1 via βPix/14-3-3/Nedd4-2 signaling affects the number of channels at the apical plasma membrane.

CONCISE METHODS

cDNA Constructs and Cell Culture

All chemicals and materials were purchased from either Fisher Scientific, Sigma, or CalBiochem unless noted otherwise. CHO and M-1 cells were obtained from ATCC and maintained with standard culture conditions (Dulbecco modified Eagle medium, 10% FBS, 1× penicillin-streptomycin, 37°C, 5% CO_2). Immortalized mouse cortical CD ($mpkCCD_{c14}$) principal cells were grown in defined medium on permeable supports (Costar Transwells; 0.4-μm pore, 24-mm diameter) or 4 × 4 glass chips as described previously.[47,48] Cells were maintained with FBS and corticosteroids, allowing them to polarize and form monolayers with high resistances and avid Na^+ reabsorption. The expression vectors encoding wild-type β_1Pix, β_1Pix (L238R, L239R), and β_1Pix (Δ602 to 611) were described previously.[27,29] The expression vectors encoding ET_BR, wild-type Rac1, and wild-type and constitutively active Cdc42 (G12V) were from the UMR cDNA Resource Center (http://www.cdna.org). The expression vector encoding constitutively active Rac1 (QL) was from Dr. A. Chan (Medical College of Wisconsin). The expression vector encoding wild-type 14-3-3β was a kind gift from Dr. M.S. Shapiro (San Antonio, TX). The vectors encoding FLAG-tagged Nedd4-2 and Liddle syndrome mutants (mutation of the three prolines, 3P; $\alpha_{P698-700A}$, $\beta_{P643-645A}$, and $\gamma_{P629-631A}$) of ENaC subunits were a kind gift from Dr. J.D. Stockand (San Antonio, TX). Dominant negative Nedd4-2 (Ser221, Thr246, and Ser327 phosphorylation sites mutated to Ala) was provided by Dr. P.M. Snyder and described previously.[49] The mammalian expression vectors encoding α-, β-, and γ-mouse ENaC and T628A mutant have been described previously.[21,40]

Isolation of CDs

Patch-clamp electrophysiology was used to assess ENaC activity in isolated, split-open rat CCD. CCDs were isolated from salt-restricted

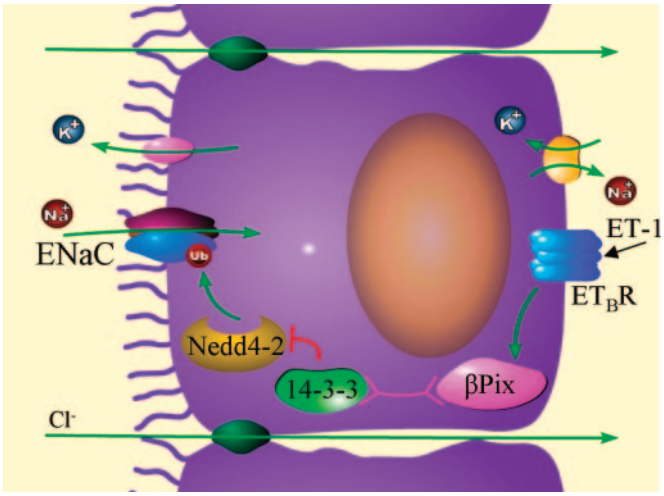

Figure 11. Schematic illustrates the proposed role for βPix in the long-term effect of ET-1 on ENaC.

(Na^+-deficient diet for 1 week) Sprague-Dawley rats to set initial ENaC activity to a high level. This preparation has been described previously.[48,50,51] Kidneys were cut into thin slices (<1 mm) with slices placed into ice-cold physiologic saline solution (pH 7.4). CDs were mechanically isolated from these slices by microdissection using forceps under a stereomicroscope. Isolated CCDs were allowed to settle onto a 5 × 5 mm coverglass coated with poly-L-lysine. Coverglasses that contained CCDs were placed within a perfusion chamber mounted on an inverted Nikon TE2000 microscope and superfused with a physiologic saline solution buffered with HEPES (pH 7.4). CCDs were split open with a sharpened micropipette controlled with a micromanipulator to gain access to the apical membrane. Animal use and welfare adhered to the National Institutes of Health "Guide for the Care and Use of Laboratory Animals" following a protocol reviewed and approved by the Institutional Animal Care and Use Committee.

Transfection

For electrophysiology experiments CHO cells were seeded on sterile 4 × 4 mm coverglass in 35-mm Petri dishes and transfected using Polyfect reagent (Qiagen, Valencia, CA) as described previously.[52] Mouse ENaC was reconstituted by coexpressing α-, β-, and γ-channel subunits together. For expression of ENaC in CHO cells, subunit cDNA transfection ratios of 1:1:1 were used (0.1 to 0.3 μg of cDNA per 35-mm dish). To define successfully transfected cells, 0.5 μg of green fluorescence protein was also added to cDNA mix.

βPix shRNA (m) lentiviral particles (subcutaneously-39149-V; Santa Cruz Biotechnology) were used for the inhibition of βPix expression in $mpkCCD_{c14}$ cells. βPix shRNA lentiviral particles are a pool of concentrated, transduction-ready viral particles containing three target-specific constructs that encode 19- to 25-nucleotide (plus hairpin) shRNA designed to knock down gene expression. Control shRNA Lentiviral Particles (subcutaneously-108080; Santa Cruz Biotechnology) were used to confirm the transduction efficiency. After transduction with Santa Cruz transfection reagent, stable cell line expressing the shRNA was isolated via selection with puromycin.

Immunohistochemistry

The Sprague-Dawley rat kidneys were fixed 24 to 48 hours in zinc formalin and processed for paraffin embedding. The kidney sections were cut at 4 μm, dried, and deparaffinized for subsequent labeled streptavidin-biotin immunohistochemistry. After deparaffinization, the slides were treated with a citrate buffer (pH 6) for a total of 35 minutes. The slides were blocked with a peroxidase block (DAKO), avidin block (Vector Labs), biotin block (Vector Labs), and serum-free protein block (DAKO). Tissue sections were incubated for 90 minutes in a 1:200 concentration of anti-βPix (Millipore). Secondary detection was performed with goat anti-rabbit biotinylated IgG (Biocare) followed by streptavidin horseradish peroxidase (Biocare) and visualized with DAB (DAKO). All slides were counterstained with a Mayer hematoxylin (DAKO), dehydrated, and mounted with permanent mounting media (Sakura).

Electrophysiology

Single-channel current data were acquired and subsequently analyzed with Axopatch 200B or MultiClamp 700B patch-clamp amplifiers (Molecular Devices, Sunnyvale, CA) interfaced via a Digidata 1440A (Molecular Devices) with a PC running the pClamp 9.0 or 10.2 suite of software. After a high-resistance seal (over 10 GOhm) was obtained, cell-attached recording was performed immediately. The membrane resistance was monitored regularly to ensure the quality of recording. For measurements of acute effect, only one experiment was performed per dish to avoid any possibility of examining cells whose properties might have been altered by extended exposure to ET-1. When currents were acquired with an Axopatch 200B amplifier, currents were filtered with an eight-pole, low-pass Bessel filter LPF-8 (Warner Institute, Hamden, CT) at 0.2 kHz. All experiments were performed at room temperature with fire-polished pipettes of borosilicate glass (World Precision Instruments, Sarasota, FL). The pipette was pulled by a horizontal puller (Sutter P-97; Sutter Instruments, Novato, CA). The resistance of the pipette in the corresponding bath medium was 7 to 12 MOhm. Typical bath solution was (in mM): 150 NaCl, 1 $CaCl_2$, 2 $MgCl_2$, and 10 HEPES (pH 7.4). Pipette solution for cell attached configuration was (in mM): 140 LiCl, 2 $MgCl_2$, and 10 HEPES (pH 7.4).

Whole-cell macroscopic current recordings of mENaCs expressed in CHO cells were made under voltage-clamp conditions using standard methods.[22,52] Cells were clamped to a 40 mV holding potential with voltage ramps (500 ms) from 60 mV down to −100 mV used to elicit current. Pipette solution for whole-cell configuration was (in mM): 120 CsCl, 5 NaCl, 2 $MgCl_2$, 5 EGTA, 2 Mg-ATP, 0.1 GTP, and 10 mM HEPES (pH 7.4). Typical bath solution was (in mM): 150 NaCl, 1 $CaCl_2$, 2 $MgCl_2$, and 10 HEPES (pH 7.4). ENaC activity was assessed as the amiloride-sensitive current density at −80 mV. Whole-cell capacitance, on average 6 to 10 pF, was compensated. Series resistances, on average 2 to 5 MOhm, were also compensated.

Single-Channel Data Analysis

All experiments were acquired using pClamp 9.0 or 10.2 software, with time and current amplitude data analyzed with this software in conjunction with Origin 7.0 (OriginLab, Northampton, MA).

Patches were selected for low baseline noise levels with no drift of the baseline current (in general, low noise was associated with high-seal resistances). Channel activity was determined during at least 1-minute recording period before application of ET-1. The channel events were analyzed by Clampfit 9.0 or 10.2 software (single-channel search in analyze function). A 50% threshold cross-method was utilized to determine valid channel openings. All events were carefully checked visually before being accepted. NP_o, the product of the number of channels and the P_o, or P_o itself, was used to measure the channel activity within a patch. Single-channel unitary current (i) was determined from the best-fit Gaussian distribution of amplitude histograms. Channel activity was analyzed as $NP_o = I/i$, where I is mean total current in a patch and i is unitary current at this voltage. By definition, then, current at the closed state is 0. When multiple-channel events were observed in a patch, the total number of functional channels (N) in the patch was determined by observing the number of peaks detected on all-point amplitude histograms at the first minute after application of ET-1 when maximum activity was observed. If channels opened independently of one another and the exact number of channels in a patch was known, then the open probability of a single channel could be calculated by dividing NP_o by the number of channels in a patch. Thus, where appropriate, P_o was calculated by normalizing NP_o for the total number of estimated channels (N) in the patch. To increase accuracy in measurement of P_o, only patches containing five channels or fewer were used.

Immunoprecipitation and Western Blot Analysis

$mpkCCD_{c14}$ or CHOs were transfected with the appropriate construct for 24 hours. Cells were washed twice in PBS and lysed in lysis buffer containing 20 mM Tris (pH 7.5), 100 mM NaCl, 5 mM $MgCl_2$, 1 mM EDTA, 1% Triton X-100, 1 mM sodium fluoride, 1 mM sodium vanadate, 1 mM phenylmethyl sulfonyl fluoride, 1 μg/ml pepstatin, and 1 μg/ml leupeptin. Equal amounts of proteins were separated by using 7.5% SDS-PAGE, electrophoretically transferred onto a polyvinylidene difluoride membrane (Millipore), immunoblotted with the appropriated antibody, and visualized by enhanced chemiluminescence (Amersham Biosciences Inc., Piscataway, NJ). For immunoprecipitation (intraperitoneally), antibodies against FLAG, 14-3-3β, or βPix (Santa Cruz Biotechnology, Santa Cruz, CA) were added to the cell lysate (500 μg) for 2-hour incubation, followed by addition of protein A or protein G agarose beads for an additional hour. The beads were washed three times in PBS. The immunoprecipitated proteins were released from the beads by boiling in 1× sample buffer for 5 minutes and subsequently were analyzed by Western blotting. Total cell lysate (Total) was run to assess the equal overexpression of the constructs. Expression of recombinant proteins was verified by immunoblotting with antibodies to the βPix. Equal amounts of cell lysate were subjected to Western blot analysis using antibodies against βPix (Chemicon, Temecula, CA), myc, or β-actin (Sigma).

Statistical Analysis

All summarized data reported as mean ± SEM; statistical analyses were performed using corresponding *t* test. For paired experiments, Wilcoxon signed-rank test was used. Differences were considered statistically significant at $P < 0.05$. ($^*P < 0.05$; $^{**}P < 0.01$; $^{***}P < 0.001$).

ACKNOWLEDGMENTS

Glen Slocum and Christine Duris are recognized for excellent technical assistance with immunohistochemistry experiments. We are grateful to Drs. Simon Prosser and David L. Mattson (Medical College of Wisconsin) for critical reading and correcting this manuscript, and Drs. Andrew Chan (Medical College of Wisconsin), Peter M. Snyder (University of Iowa), and James D. Stockand (University of Texas Health Science Center at San Antonio) for providing constructs used in this study. This research was supported by the National Institutes of Health grants HL022563 and DK041684 (to A. Sorokin), American Heart Association grants SDG 0730111N (to A. Staruschenko) and 09SDG2230391 (to O.P.), and a Carl W. Gottschalk Research Scholar Grant from the American Society of Nephrology (to A. Staruschenko). Part of this work was presented at the Experimental Biology Meeting, New Orleans, LA, April 18 to 22, 2009; the ET-11: APS International Conference on Endothelin, Montreal, Canada, September 9 to 12, 2009; and the American Society of Nephrology Meeting, San Diego, CA, October 27 to November 1, 2009.

DISCLOSURES

None.

REFERENCES

1. Bhalla V, Hallows KR: Mechanisms of ENaC regulation and clinical implications. *J Am Soc Nephrol* 19: 1845–1854, 2008
2. Schild L: The epithelial sodium channel: from molecule to disease. *Rev Physiol Biochem Pharmacol* 151: 93–107, 2004
3. Strautnieks SS, Thompson RJ, Gardiner RM, Chung E: A novel splice-site mutation in the gamma subunit of the epithelial sodium channel gene in three pseudohypoaldosteronism type 1 families. *Nat Genet* 13: 248–250, 1996
4. Chang SS, Grunder S, Hanukoglu A, Rosler A, Mathew PM, Hanukoglu I, Schild L, Lu Y, Shimkets RA, Nelson-Williams C, Rossier BC, Lifton RP: Mutations in subunits of the epithelial sodium channel cause salt wasting with hyperkalaemic acidosis, pseudohypoaldosteronism type 1. *Nat Genet* 12: 248–253, 1996
5. Malik B, Price SR, Mitch WE, Yue Q, Eaton DC: Regulation of epithelial sodium channels by the ubiquitin-proteasome proteolytic pathway. *Am J Physiol Renal Physiol* 290: F1285–F1294, 2006
6. Shimkets RA, Warnock DG, Bositis CM, Nelson-Williams C, Hansson JH, Schambelan M, Gill JR Jr., Ulick S, Milora RV, Findling JW, Canessa CM, Rossier BC, Lifton RP: Liddle's syndrome: Heritable human hypertension caused by mutations in the beta subunit of the epithelial sodium channel. *Cell* 79: 407–414, 1994
7. Hansson JH, Nelson-Williams C, Suzuki H, Schild L, Shimkets R, Lu Y, Canessa C, Iwasaki T, Rossier B, Lifton RP: Hypertension caused by a truncated epithelial sodium channel gamma subunit: Genetic heterogeneity of Liddle syndrome. *Nat Genet* 11: 76–82, 1995
8. Yanagisawa M, Kurihara H, Kimura S, Tomobe Y, Kobayashi M, Mitsui Y, Yazaki Y, Goto K, Masaki T: A novel potent vasoconstrictor peptide produced by vascular endothelial cells. *Nature* 332: 411–415, 1988
9. Strait KA, Stricklett PK, Kohan JL, Miller MB, Kohan DE: Calcium regulation of endothelin-1 synthesis in rat inner medullary collecting duct. *Am J Physiol Renal Physiol* 293: F601–F606, 2007
10. Simonson MS: Endothelins: multifunctional renal peptides. *Physiol Rev* 73: 375–411, 1993

11. Sorokin A, Kohan DE: Physiology and pathology of endothelin-1 in renal mesangium. *Am J Physiol Renal Physiol* 285: F579–F589, 2003
12. Ge Y, Bagnall A, Stricklett PK, Strait K, Webb DJ, Kotelevtsev Y, Kohan DE: Collecting duct-specific knockout of the endothelin B receptor causes hypertension and sodium retention. *Am J Physiol Renal Physiol* 291: F1274–F1280, 2006
13. Ge Y, Stricklett PK, Hughes AK, Yanagisawa M, Kohan DE: Collecting duct-specific knockout of the endothelin A receptor alters renal vasopressin responsiveness, but not sodium excretion or blood pressure. *Am J Physiol Renal Physiol* 289: F692–F698, 2005
14. Ahn D, Ge Y, Stricklett PK, Gill P, Taylor D, Hughes AK, Yanagisawa M, Miller L, Nelson RD, Kohan DE: Collecting duct-specific knockout of endothelin-1 causes hypertension and sodium retention. *J Clin Invest* 114: 504–511, 2004
15. Ge Y, Bagnall A, Stricklett PK, Webb D, Kotelevtsev Y, Kohan DE: Combined knockout of collecting duct endothelin A and B receptors causes hypertension and sodium retention. *Am J Physiol Renal Physiol* 295: F1635–F1640, 2008
16. Gariepy CE, Ohuchi T, Williams SC, Richardson JA, Yanagisawa M: Salt-sensitive hypertension in endothelin-B receptor-deficient rats. *J Clin Invest* 105: 925–933, 2000
17. Gallego MS, Ling BN: Regulation of amiloride-sensitive Na+ channels by endothelin-1 in distal nephron cells. *Am J Physiol* 271: F451–F460, 1996
18. Gilmore ES, Stutts MJ, Milgram SL: SRC family kinases mediate epithelial Na+ channel inhibition by endothelin. *J Biol Chem* 276: 42610–42617, 2001
19. Bugaj V, Pochynyuk O, Mironova E, Vandewalle A, Medina JL, Stockand JD: Regulation of the epithelial Na+ channel by endothelin-1 in rat collecting duct. *Am J Physiol Renal Physiol* 295: F1063–F1070, 2008
20. Stow LR, Gumz ML, Lynch IJ, Greenlee MM, Rudin A, Cain BD, Wingo CS: Aldosterone modulates steroid receptor binding to the endothelin-1 gene (edn1). *J Biol Chem* 284: 30087–30096, 2009
21. Karpushev AV, Levchenko V, Pavlov TS, Lam VY, Vinnakota KC, Vandewalle A, Wakatsuki T, Staruschenko A: Regulation of ENaC expression at the cell surface by Rab11. *Biochem Biophys Res Commun* 377: 521–525, 2008
22. Pochynyuk O, Medina J, Gamper N, Genth H, Stockand JD, Staruschenko A: Rapid translocation and insertion of the epithelial Na+ channel in response to RhoA signaling. *J Biol Chem* 281: 26520–26527, 2006
23. Pochynyuk O, Stockand JD, Staruschenko A: Ion channel regulation by Ras, Rho, and Rab small GTPases. *Exp Biol Med (Maywood)* 232: 1258–1265, 2007
24. Pochynyuk O, Staruschenko A, Bugaj V, Lagrange L, Stockand JD: Quantifying RhoA facilitated trafficking of the epithelial Na+ channel toward the plasma membrane with total internal reflection fluorescence-fluorescence recovery after photobleaching. *J Biol Chem* 282: 14576–14585, 2007
25. Staruschenko A, Nichols A, Medina JL, Camacho P, Zheleznova NN, Stockand JD: Rho small GTPases activate the epithelial Na(+) channel. *J Biol Chem* 279: 49989–49994, 2004
26. Staruschenko A, Patel P, Tong Q, Medina JL, Stockand JD: Ras activates the epithelial Na(+) channel through phosphoinositide 3-OH kinase signaling. *J Biol Chem* 279: 37771–37778, 2004
27. Chahdi A, Miller B, Sorokin A: Endothelin 1 induces beta 1Pix translocation and Cdc42 activation via protein kinase A-dependent pathway. *J Biol Chem* 280: 578–584, 2005
28. Chahdi A, Sorokin A: Endothelin 1 stimulates beta1Pix-dependent activation of Cdc42 through the G(salpha) pathway. *Exp Biol Med (Maywood)* 231: 761–765, 2006
29. Chahdi A, Sorokin A: Endothelin-1 couples betaPix to p66Shc: Role of betaPix in cell proliferation through FOXO3a phosphorylation and p27kip1 down-regulation independently of Akt. *Mol Biol Cell* 19: 2609–2619, 2008
30. Jin J, Smith FD, Stark C, Wells CD, Fawcett JP, Kulkarni S, Metalnikov P, O'Donnell P, Taylor P, Taylor L, Zougman A, Woodgett JR, Langeberg LK, Scott JD, Pawson T: Proteomic, functional, and domain-based analysis of in vivo 14-3-3 binding proteins involved in cytoskeletal regulation and cellular organization. *Curr Biol* 14: 1436–1450, 2004
31. Angrand PO, Segura I, Volkel P, Ghidelli S, Terry R, Brajenovic M, Vintersten K, Klein R, Superti-Furga G, Drewes G, Kuster B, Bouwmeester T, cker-Palmer A: Transgenic mouse proteomics identifies new 14-3-3-associated proteins involved in cytoskeletal rearrangements and cell signaling. *Mol Cell Proteomics* 5: 2211–2227, 2006
32. Chahdi A, Sorokin A: Protein kinase A-dependent phosphorylation modulates beta1Pix guanine nucleotide exchange factor activity through 14-3-3beta binding. *Mol Cell Biol* 28: 1679–1687, 2008
33. Bhalla V, Daidie D, Li H, Pao AC, LaGrange LP, Wang J, Vandewalle A, Stockand JD, Staub O, Pearce D: Serum- and glucocorticoid-regulated kinase 1 regulates ubiquitin ligase neural precursor cell-expressed, developmentally down-regulated protein 4-2 by inducing interaction with 14-3-3. *Mol Endocrinol* 19: 3073-3084, 2005
34. Ichimura T, Yamamura H, Sasamoto K, Tominaga Y, Taoka M, Kakiuchi K, Shinkawa T, Takahashi N, Shimada S, Isobe T: 14-3-3 proteins modulate the expression of epithelial Na+ channels by phosphorylation-dependent interaction with Nedd4-2 ubiquitin ligase. *J Biol Chem* 280: 13187–13194, 2005
35. Liang X, Peters KW, Butterworth MB, Frizzell RA: 14-3-3 isoforms are induced by aldosterone and participate in its regulation of epithelial sodium channels. *J Biol Chem* 281: 16323–16332, 2006
36. Liang X, Butterworth MB, Peters KW, Walker WH, Frizzell RA: An obligatory heterodimer of 14-3-3beta and 14-3-3epsilon is required for aldosterone regulation of the epithelial sodium channel. *J Biol Chem* 283: 27418–27425, 2008
37. Nagaki K, Yamamura H, Shimada S, Saito T, Hisanaga S, Taoka M, Isobe T, Ichimura T: 14-3-3 Mediates phosphorylation-dependent inhibition of the interaction between the ubiquitin E3 ligase Nedd4-2 and epithelial Na+ channels. *Biochemistry* 45: 6733–6740, 2006
38. Manser E, Loo TH, Koh CG, Zhao ZS, Chen XQ, Tan L, Tan I, Leung T, Lim L: PAK kinases are directly coupled to the PIX family of nucleotide exchange factors. *Mol Cell* 1: 183–192, 1998
39. Bagrodia S, Bailey D, Lenard Z, Hart M, Guan JL, Premont RT, Taylor SJ, Cerione RA: A tyrosine-phosphorylated protein that binds to an important regulatory region on the cool family of p21-activated kinase-binding proteins. *J Biol Chem* 274: 22393–22400, 1999
40. Staruschenko A, Pochynyuk O, Stockand JD: Regulation of epithelial Na+ channel activity by conserved serine/threonine switches within sorting signals. *J Biol Chem* 280: 39161–39167, 2005
41. Yang LM, Rinke R, Korbmacher C: Stimulation of the epithelial sodium channel (ENaC) by cAMP involves putative ERK phosphorylation sites in the C termini of the channel's beta- and gamma-subunit. *J Biol Chem* 281: 9859–9868, 2006
42. Shi H, Asher C, Chigaev A, Yung Y, Reuveny E, Seger R, Garty H: Interactions of beta and gamma ENaC with Nedd4 can be facilitated by an ERK-mediated phosphorylation. *J Biol Chem* 277: 13539–13547, 2002
43. Debonneville C, Flores SY, Kamynina E, Plant PJ, Tauxe C, Thomas MA, Munster C, Chraibi A, Pratt JH, Horisberger JD, Pearce D, Loffing J, Staub O: Phosphorylation of Nedd4-2 by Sgk1 regulates epithelial Na(+) channel cell surface expression. *EMBO J* 20: 7052–7059, 2001
44. Fejes-Toth G, Frindt G, Naray-Fejes-Toth A, Palmer LG: Epithelial Na+ channel activation and processing in mice lacking SGK1. *Am J Physiol Renal Physiol* 294: F1298–F1305, 2008
45. Snyder PM, Olson DR, Thomas BC: Serum and glucocorticoid-regulated kinase modulates Nedd4-2-mediated inhibition of the epithelial Na+ channel. *J Biol Chem* 277: 5–8, 2002

46. Raikwar NS, Thomas CP: Nedd4-2 isoforms ubiquitinate individual epithelial sodium channel subunits and reduce surface expression and function of the epithelial sodium channel. *Am J Physiol Renal Physiol* 294: F1157–F1165, 2008
47. Bens M, Vallet V, Cluzeaud F, Pascual-Letallec L, Kahn A, Rafestin-Oblin ME, Rossier BC, Vandewalle A: Corticosteroid-dependent sodium transport in a novel immortalized mouse collecting duct principal cell line. *J Am Soc Nephrol* 10: 923–934, 1999
48. Staruschenko A, Pochynyuk O, Vandewalle A, Bugaj V, Stockand JD: Acute regulation of the epithelial Na+ channel by phosphatidylinositide 3-OH kinase signaling in native collecting duct principal cells. *J Am Soc Nephrol* 18: 1652–1661, 2007
49. Kabra R, Knight KK, Zhou R, Snyder PM: Nedd4-2 induces endocytosis and degradation of proteolytically cleaved epithelial Na+ channels. *J Biol Chem* 283: 6033–6039, 2008
50. Sun P, Lin DH, Wang T, Babilonia E, Wang Z, Jin Y, Kemp R, Nasjletti A, Wang WH: Low Na intake suppresses expression of CYP2C23 and arachidonic acid-induced inhibition of ENaC. *Am J Physiol Renal Physiol* 291: F1192–F1200, 2006
51. Wei Y, Sun P, Wang Z, Yang B, Carroll MA, Wang WH: Adenosine inhibits ENaC via cytochrome P-450 epoxygenase-dependent metabolites of arachidonic acid. *Am J Physiol Renal Physiol* 290: F1163–F1168, 2006
52. Staruschenko A, Booth RE, Pochynyuk O, Stockand JD, Tong Q: Functional reconstitution of the human epithelial Na+ channel in a mammalian expression system. *Methods Mol Biol* 337: 3–13, 2006